

## FIRST RESULTS FROM THE GODDARD HIGH-RESOLUTION SPECTROGRAPH: RESOLVED VELOCITY AND DENSITY STRUCTURE IN THE $\beta$ PICTORIS CIRCUMSTELLAR GAS

A. BOGGESS,<sup>1,2</sup> FREDERICK C. BRUHWEILER,<sup>3,4,5</sup> C. A. GRADY,<sup>3,5</sup> DENNIS C. EBBETS,<sup>1,6</sup> YOJI KONDO,<sup>2</sup>  
 L. M. TRAFTON,<sup>1,7</sup> JOHN C. BRANDT,<sup>1,8</sup> AND S. R. HEAP<sup>1,2</sup>

Received 1991 March 29; accepted 1991 May 20

### ABSTRACT

We present the first *HST* Goddard High-Resolution Spectrograph (GHRS) observations of circumstellar (CS) gas around  $\beta$  Pictoris, providing the first evidence for resolved velocity *and* density structure in the CS gas. Two low-density features are visible in both observations. Comparison with *IUE* spectra suggests that at least one component may vary on time scales longer than the 23 day interval between the *HST* observations, implying that some of the low-density gas is CS. The high-density, infalling gas shows considerable velocity structure which varied dramatically between the two *HST* observations. The *HST* and *IUE* data are consistent with 2–3 infalling clumps of material per week. We infer an infall rate of 100–150 events  $\text{yr}^{-1}$ , a rate which is broadly consistent with, but higher than, previously inferred infall rates. Collectively the GHRS data imply the presence of a more complex and dynamically active gaseous envelope than previously anticipated.

*Subject headings:* interstellar: matter — stars: circumstellar shells — stars: individual (HD 39060) — ultraviolet: spectra

### 1. INTRODUCTION

The star,  $\beta$  Pic, has excited considerable interest as a candidate proto-planetary system since the detection of circumstellar (CS) dust emission by the *Infrared Astronomy Satellite* (*IRAS*) (Aumann et al. 1984; Aumann 1985), and subsequent imaging of an extended disk (Smith & Terrile 1984, 1987; Paresce & Burrows 1987; Telesco et al. 1988). The detection of both a central cavity in the dust disk (Telesco et al. 1988) and episodes of infalling high-density gas (Kondo & Bruhweiler 1985; Hobbs 1986; Lagrange et al. 1987; Lagrange-Henri et al. 1988) has reinforced this interpretation. The infalling gas is now known to be dramatically variable in infall velocity and mass infall rate (Bruhweiler, Kondo, & Grady 1991; Lagrange-Henri et al. 1988). Sporadic detections of mass outflow imply that some of the CS gas may be stellar ejecta (Bruhweiler et al. 1991). Collectively, these studies suggest that the spatial distribution of the gas and its kinematics within 1–2 AU of  $\beta$  Pic are complex.

We present the first *Hubble Space Telescope* (*HST*) Goddard High-Resolution Spectrograph (GHRS) observations of the gas around  $\beta$  Pictoris. These data, representing a significant enhancement in velocity resolution and in signal-to-noise (S/N) ratios over previous UV studies of this star, allow

us, for the first time, to probe the density and velocity structure of the CS gas simultaneously.

### 2. OBSERVATIONS AND DATA REDUCTION

#### 2.1. Observations

The star  $\beta$  Pictoris was observed with the *HST* GHRS on 1991 January 12 and February 4 as part of the Early Release Observation Program. The first observation was performed using an interactive acquisition, while the flight software performed the acquisition autonomously for the second observation. Spectra were then taken with the star in both the 2"0 Large Science Aperture (LSA) and with the star precisely centered in the 0"25 Small Science Aperture (SSA). Since the SSA spectra offer superior spectral resolution, the remainder of our paper is devoted to them. Our data include moderate resolution G270M spectra spanning the wavelength range 2579–2626 Å, covering the UV (1) multiplet of Fe II, and 2726–2772 Å covering the Fe II multiplets UV(62) and UV(63) with a resolution of  $\approx 15 \text{ km s}^{-1}$ . Echelle-B spectra from orders 22 and 21, covering 2595–2608 Å and 2733–2745 Å, with a resolution of  $3 \text{ km s}^{-1}$  (Table 1) were also obtained. The GHRS data were obtained using the FP-SPLIT option to minimize the effects of instrumental sources of fixed-pattern noise. The operation of the GHRS instrument is described by Duncan & Ebbets (1989).

#### 2.2. Data Reduction

The spectral data were background subtracted and corrected for nonuniform sensitivity of the diode array, and spectral bins were merged to form the net spectra. No correction has been made for vignetting, the echelle blaze function, or for the flux sensitivity. Small-scale photocathode sensitivity variations were compensated for by registering the subexposures in each FP-SPLIT observation to the initial spectrum, then interpolating the data to a common wavelength scale before summing to produce the final spectra. Vacuum wavelength scales were computed using dispersion constants based on internal calibration lamp spectra obtained immediately before

<sup>1</sup> Goddard High-Resolution Spectrograph (GHRS) Investigation Definition Team.

<sup>2</sup> Code 440 (A.B.; 684, Y. K.; 681, S. R. H.), NASA/GSFC, Greenbelt, MD 20771.

<sup>3</sup> Department of Physics, The Catholic University of America, Washington, DC 20064.

<sup>4</sup> Goddard High-Resolution Spectrograph Science Support Group/CSC.

<sup>5</sup> Guest Observer, *International Ultraviolet Explorer* (*IUE*) Observatory, operated by Goddard Space Flight Center, National Aeronautics and Space Administration.

<sup>6</sup> Ball Aerospace Systems Group, P.O. Box 1062, JWF-3, Boulder, CO 80306.

<sup>7</sup> MacDonald Observatory and Astronomy Department, University of Texas, Austin, TX 78712.

<sup>8</sup> Laboratory for Atmospheric and Space Physics, Campus Box 392, University of Colorado, Boulder, CO 80309.

TABLE 1  
JOURNAL OF *HST* GHRS OBSERVATIONS

Observation Identification	Date (1991)	Grating	Midpoint (UT)	Duration (s)	$\lambda_{\text{Central}}$ (Å)	$\lambda_{\text{S/N}}$ (Å)	S/N
ZODJB20C .....	Jan 12	G270M	07:43:17	218	2603.0	2602.10	100
ZODJB20E .....	Jan 12	G270M	07:50:18	109	2750.0	2738.50	60
ZODJB20I .....	Jan 12	Ech-B	08:16:07	1088	2602.9	2599.35	34
ZODJB20M .....	Jan 12	Ech-B	09:46:36	2176	2740.1	2739.55	67
ZODJ020B .....	Feb 4	G270M	14:11:32	218	2603.0	2602.10	87
ZODJ020D .....	Feb 4	G270M	14:18:32	109	2750.0	2738.50	53
ZODJ020H .....	Feb 4	Ech-B	14:44:22	1088	2602.9	2599.10	28
ZODJ020J .....	Feb 4	Ech-B	16:17:07	2176	2740.1	2739.55	66

the science observations and at the same grating carousel positions. The wavelength data were converted to heliocentric, air wavelengths. No correction has been made for the stellar radial velocity due to the large range of published values.

The UV spectrum of  $\beta$  Pic is dominated by rotationally broadened photospheric features with superposed absorption cores due to interstellar and CS gas (Slettebak & Carpenter 1983). The echelle spectra have  $S/N \geq 25$  adjacent to the absorption cores. Precise centering of the star in the SSA, together with use of the internal wavelength calibration spectra, ensures that the wavelength scales of the GHRS data are accurate to  $\approx 0.25$  diodes, corresponding to  $\approx 0.6 \text{ km s}^{-1}$  for the echelle spectra. The combination of high S/N ratios, accurate radial velocities, and preservation of line profile information permits both clean separation of the CS absorption from the photospheric spectrum and confident detection of weak discrete features.

### 3. THE LINE PROFILES

The remainder of our study is devoted to the absorption cores of three spectral lines which are typical of other lines in their multiplets: Fe II (UV1)  $\lambda 2599.395$ ,  $\lambda 2598.37$ , and Fe II (UV 63)  $\lambda 2739.546$  (Fig. 1). The  $\lambda 2598.37$  and  $\lambda 2739.546$  lines are sensitive only to densities greatly in excess of densities (e.g.,  $n \approx 0.1 \text{ cm}^{-3}$ ; Bruhweiler & Vidal-Madjar 1987) typical of the Local Interstellar Medium (Kondo & Bruhweiler 1985),

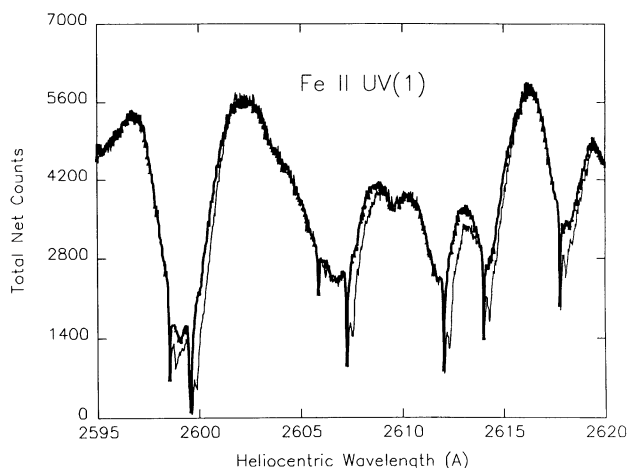


FIG. 1.—A portion of the G270M, SSA spectra of  $\beta$  Pic showing several Fe II UV (1) lines. The 1991 Feb 4 spectrum (*light line*) is scaled by 120% to compensate for the enhanced spacecraft pointing jitter and plotted with the 1991 Jan 12 spectrum (*bold*). On Feb. 4, all of the Fe II lines show excess absorption longward of the line centers, which can be followed in the echelle data to  $+220 \text{ km s}^{-1}$ .

whereas the  $\lambda 2599.396$  line is insensitive to density. Comparison of the absorption profiles in these lines allows us to probe the density structure of gas in the line of sight to  $\beta$  Pic, at the same time that the superior velocity resolution of the GHRS enables us to map the distribution of gas as a function of radial velocity. Due to the complexity of the observed line profiles, we present only a qualitative discussion of the GHRS spectra in this paper, with quantitative analysis of the individual features deferred to a follow-on study.

#### 3.1. Fe II $\lambda 2599.396$

The Fe II  $\lambda 2599.396$  line arises from the zero V level of the ground configuration and thus has both interstellar and CS contributions (Kondo & Bruhweiler 1985). The echelle spectra (Fig. 2) show that the line is resolved into at least four components. The 1991 January 12 spectrum has a narrow component with a velocity of  $10.3 \text{ km s}^{-1}$ , a broader feature, with saturated absorption extending from  $18$ – $29 \text{ km s}^{-1}$ , and a longward-asymmetric wing extending to  $\approx 50 \text{ km s}^{-1}$ . There is some suggestion of an extremely weak absorption near  $70 \text{ km s}^{-1}$ . On February 4, the sharp  $10.3 \text{ km s}^{-1}$  component and saturated absorption were unchanged. However, the longward-asymmetric wing was much stronger and extended to  $220 \text{ km s}^{-1}$  (Fig. 1). Two new features were superposed on this wing: a sharp component (FWHM =  $3 \text{ km s}^{-1}$ ) at  $33 \text{ km s}^{-1}$ , and a broader feature, (FWHM =  $24 \text{ km s}^{-1}$ ) at  $52 \text{ km s}^{-1}$ .

#### 3.2. Fe II $\lambda 2598.37$

This line, also a member of the UV1 resonance multiplet, comes from an excited  $J$ -level some  $385 \text{ cm}^{-1}$  above ground. A minimum density of  $\approx 10^3 \text{ cm}^{-3}$  is needed to produce appreciable absorption in this line, which thus provides a probe of the intermediate-density CS gas (Kondo & Bruhweiler 1985). The  $\lambda 2598.37$  profiles differ from the Fe II  $\lambda 2599.396$  profiles in the absence of both the  $10.3$  and  $28 \text{ km s}^{-1}$  features. The saturated absorption present in the  $\lambda 2599.396$  line is reduced to a feature centered at  $20.4 \text{ km s}^{-1}$ . The variation between 11 January and 4 February mirrors the behavior of the  $\lambda 2599.396$  line.

#### 3.3. Fe II $\lambda 2739.546$

Absorption can be seen arising from the metastable  $^4D$  level of Fe II,  $\approx 1.05 \text{ eV}$  above ground, only if  $n \geq 10^{8-9} \text{ cm}^{-3}$  (Kondo & Bruhweiler 1985; Bruhweiler et al. 1991). The velocity structure visible in this and other lines of UV (62) and UV (63) of Fe II is similar to the  $\lambda 2598.37$  line (Fig. 2). On February 4 the longward-asymmetric profile wing is visible to  $\approx 190 \text{ km s}^{-1}$ .

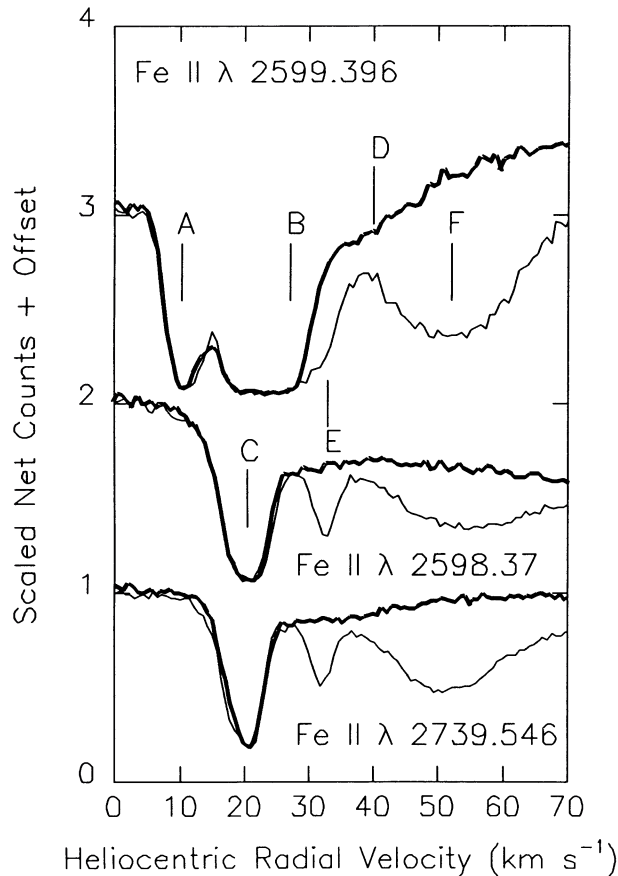


FIG. 2.—Velocity and density structure in the Interstellar and CS Fe II line profiles. The 1991 Jan 12 profiles (**bold**) are characterized by two low-density components at 10.3 (denoted by “A”) and 28 (“B”)  $\text{km s}^{-1}$ , as well as a broad, high-density feature, “C,” centered at 20.4  $\text{km s}^{-1}$  and visible in  $\lambda\lambda 2599.396$ , 2598.37, and 2739.546. Infalling material extending to +50  $\text{km s}^{-1}$  (heliocentric) is visible as a longward-asymmetric wing to the profile (“D”). On 1991 Feb 4 (*light line*) components A–C are still present, but are supplemented by a high-density feature at +33  $\text{km s}^{-1}$  (“E”) and a broad component at +52  $\text{km s}^{-1}$  (“F”). The nonzero flux in the absorption trough in the  $\lambda 2599.396$  profile is due to the 2.5% scattered light (Cardelli et al. 1991).

#### 4. COMPARISON WITH NEAR-SIMULTANEOUS AND ARCHIVAL *IUE* DATA

High-dispersion *IUE* long-wavelength spectra of  $\beta$  Pic were obtained on 1991 January 11, 23:57 UT (LWP 19548), and 1991 February 9, 20:20 UT (LWP 18723), permitting us to relate the structure in the *HST* data to *IUE* archival spectra. The *IUE* profiles of the Fe II 2599.396 Å feature agree well, to within the S/N ratio of the *IUE* data, with heavily smoothed GHRS data. Comparison of our spectra with archival data indicates that more gas was in the line of sight to  $\beta$  Pic on 1991 January 11 and February 9 than in the minimum absorption state (LWP 8132, Bruhweiler et al. 1991), with additional absorption present shortward of the CS feature. This suggests that the low-density absorption may vary on time scales longer than  $\approx 3$  weeks.

#### 5. DISCUSSION

##### 5.1. Location of the Low-Density Gas

The GHRS data for early 1991 indicate the presence of two features with  $n < 10^3 \text{ cm}^{-3}$  in the line of sight to  $\beta$  Pic. These

components can be produced either in the Local Interstellar Medium, or close to the star. Applying Crutcher’s (1982) relation to predict the interstellar wind velocity, we would expect a component at 16.6  $\text{km s}^{-1}$  for  $\beta$  Pic ( $l = 258^\circ 37$ ,  $b = -30^\circ 61$ ), in disagreement with the velocity of either low-density component. While multiple interstellar velocity components are observed toward other nearby stars (Lallement, Vidal-Madjar, & Ferlet 1986), the excess absorption noted in our *IUE* data suggests that the 10.3  $\text{km s}^{-1}$  feature may be variable and hence, CS. If correct, the high-density CS gas surrounding  $\beta$  Pic may be embedded in an extended, low-density gaseous halo.

##### 5.2. The Infalling Gas

To date, the bulk of the attention devoted to the CS gas has been focused on absorption features with large positive velocities. Based on numerous detections of such features, together with the comparative rarity of detections of gas which is shortward-shifted relative to the +20.4  $\text{km s}^{-1}$  feature, these features have been interpreted as evidence for gas falling toward the star (Lagrange et al. 1987; Lagrange-Henri et al. 1988). The GHRS spectra show evidence for infalling gas at times when comparison with the *IUE* data suggests a comparatively quiescent gas envelope. Thus, the GHRS data imply that infall features, particularly those involving small column densities, are common. The persistence of the +52  $\text{km s}^{-1}$  feature from February 4–9, when it was detected by *IUE* as enhanced absorption on the wing of the CS core, together with the variability in the high-velocity components, suggests that features at  $\approx 50 \text{ km s}^{-1}$  may be visible for approximately 1 week. The detection of 2–3 infalling components per observation implies that the infalling material is quite clumpy. If such components persist for a week, the data imply  $\approx 100$ –150 infall events  $\text{yr}^{-1}$ , a rate broadly consistent with, but somewhat higher than, the infall rate suggested by Lagrange-Henri et al. (1988).

##### 5.3. Toward a Physical Model for the CS Gas Surrounding $\beta$ Pic

We propose a speculative model for the spectral phenomena (Fig. 3). In our model, most of the high-density CS gas lies in a ring residing well within the inner boundary of the dust disk and in Keplerian orbit about the star (“C” in Figs. 2 and 3). How the gas in this ring is maintained is unclear. Possibilities include steady erosion of the surrounding dust disk (Smith & Terrile 1984), by cometary bodies passing near the star (Lagrange-Henri et al. 1988), or even by mass ejection events from the star itself (Bruhweiler et al. 1991). Viscous forces or instabilities in the ring presumably trigger further infall, either as prolonged, uniform, steady flows, or in surges. Steady infall could produce the longward-asymmetric wings to the Fe II profiles (“D”). The surges produce denser streams, resulting in the discrete features superposed upon the profile wings. The surges develop wider velocity dispersions as they fall down the stellar gravitational well, which is manifested as a systematic broadening of the discrete components with increasing velocity (“E” and “F”). The location of the low-density gas (“A” and “B”) in our model is uncertain. The *IUE* data suggest that the 10.3  $\text{km s}^{-1}$  feature is more likely to be CS, so we tentatively associate this component with the expanding halo inferred from archival *IUE* spectra (Bruhweiler et al. 1991). We emphasize that our model is quite speculative. Currently the major uncertainty is the relationship between the gas ring, dust disk,

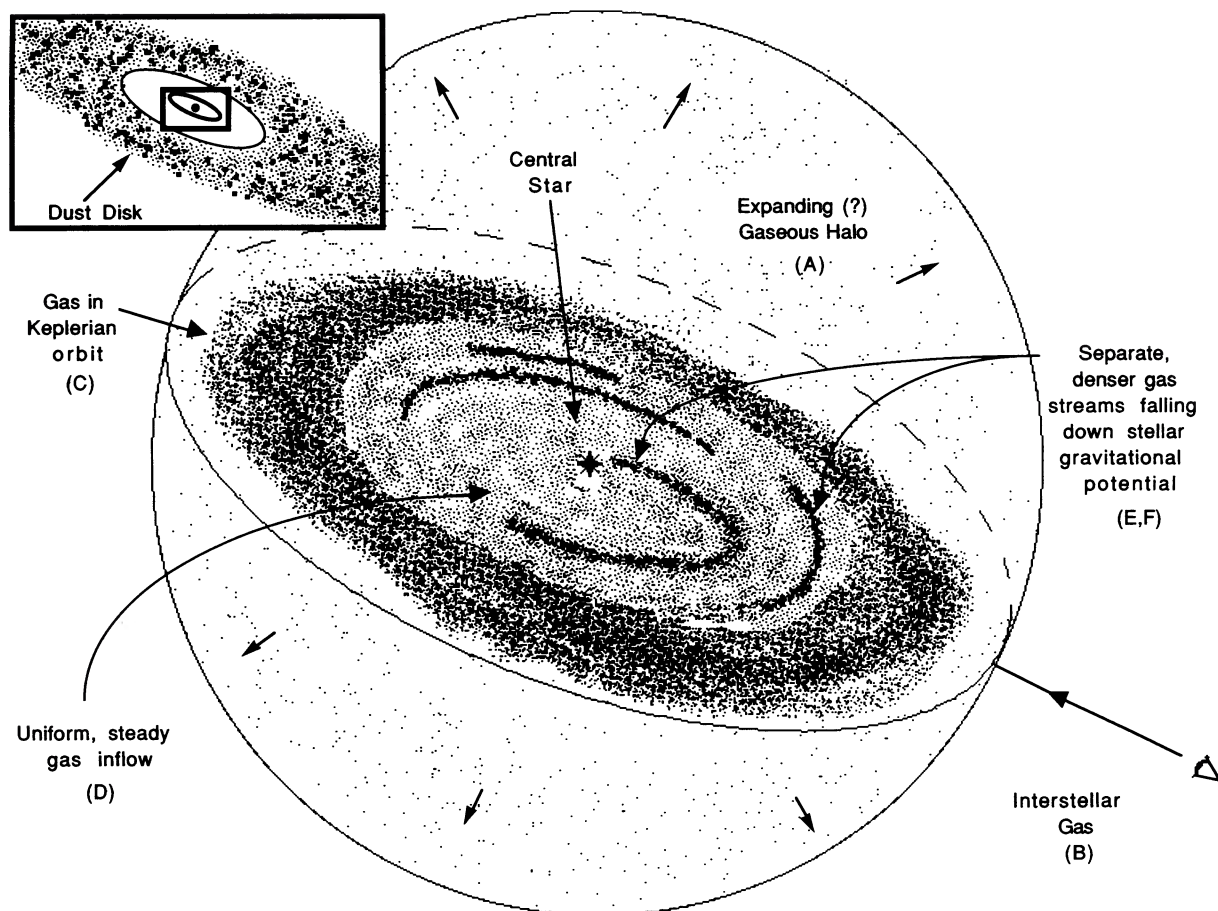


FIG. 3.—Artist's concept of the near-stellar environment of  $\beta$  Pic. Inset shows our suggested location for the CS gas ring ("C") well within the inner boundary of the CS dust disk. The CS gas ring surrounds a region of both uniform, steady gas inflow ("D") and separate, denser streams which are falling down the stellar gravitational potential well ("E," "F"). The low-density components may be located in the expanding gaseous halo inferred from *IUE* observations ("A," "B") or may be foreground features due to the Local Interstellar Medium.

stellar ejecta, and the location of the Al III detected in *IUE* spectra (Lagrange-Henri et al. 1988).

The excellent velocity resolution, accurate wavelength scales, and high S/N ratios of our GHRIS data have permitted us to probe the CS gas structure within 1–2 AU of  $\beta$  Pic with unprecedented sensitivity. As we have discovered with these observations, the gaseous disk of  $\beta$  Pic is far more complicated than we had first envisioned, and future observations should harbor additional surprises.

We wish to thank the staff of the STScI, especially in OSS, as well as H. Garner, J. Troeltzsch, C. Peck, and J. Kinsey of the BASG, D. Norman of CSC, J. K. Feggans of ACC, and J. M. S. Silvis of CUA for providing invaluable support for this study. The *IUE* observations were obtained under a grant of Director's discretionary time, and were scheduled with little advance notice. Computer resources for the *IUE* data analysis were provided by the *IUE* RDAF at GSFC.

#### REFERENCES

- Aumann, H. H. 1985, *BAAS*, 16, 483  
 Aumann, H. H., et al. 1984, *ApJ*, 278, L23  
 Bruhweiler, F. C., Kondo, Y., & Grady, C. A. 1991, *ApJ*, 371, L27  
 Bruhweiler, F. C., & Vidal-Madjar, A. 1987, *The Interstellar Medium Near the Sun*, in *Exploring the Universe with the IUE Satellite*, ed. Y. Kondo (Dordrecht: Reidel), 467  
 Cardelli, J. A., et al. 1991, *ApJ*, 377, L61  
 Crutcher, R. M. 1982, *ApJ*, 254, 82  
 Duncan, D. K., & Ebbets, D. 1989, *Hubble Space Telescope Goddard High-Resolution Spectrograph Instrument Handbook (Version 2.0)* (Baltimore: Space Telescope Science Institute)  
 Ferlet, R., Hobbs, L. M., & Vidal-Madjar, A. 1987, *A&A*, 185, 267  
 Hobbs, L. M. 1986, *ApJ*, 308, 854  
 Kondo, Y., & Bruhweiler, F. C. 1985, *ApJ*, 293, L1  
 Lagrange, A. M., Ferlet, R., & Vidal-Madjar, A. 1987, *A&A*, 173, 289  
 Lagrange-Henri, A. M., Vidal-Madjar, A., & Ferlet, R. 1988, *A&A*, 190, 275  
 Lallemand, R., Vidal-Madjar, A. M., & Ferlet, R. 1986, *A&A*, 168, 225  
 Paresce, F., & Burrows, C. 1987, *ApJ*, 319, L23  
 Slettebak, A., & Carpenter, K. G. 1983, *ApJ*, 53, 869  
 Smith, B. A., & Terrile, R. J. 1984, *Science*, 226, 1421  
 ———. 1987, *BAAS*, 19, 829  
 Telesco, C. M., Becklin, R. E., Wolstencroft, R. D., & Decher, R. 1988, *Nature*, 335, 51  
 Vidal-Madjar, A., Hobbs, L. M., Ferlet, R., Gry, C., & Albert, C. E. 1986, *A&A*, 167, 325